Kinase-activity-independent functions of atypical protein kinase C in *Drosophila*

Soya Kim[1,*], Ieva Gailite[1], Bernard Moussian[2], Stefan Luschnig[2,3], Maik Goette[4], Karen Fricke[1], Mona Honemann-Capito[1], Helmut Grubmüller[4] and Andreas Wodarz[1,‡]

[1]Department of Stem Cell Biology, DFG Research Center for Molecular Physiology of the Brain (CMPB), Georg-August-University Göttingen, Justus-von-Liebig-Weg 11, 37077 Göttingen, Germany
[2]Department of Genetics, Max-Planck-Institute for Developmental Biology, Spemannstrasse 35-39, 72076 Tübingen, Germany
[3]Institute of Zoology, University of Zürich, Winterthurer Strasse 190, 8057 Zürich, Switzerland
[4]Theoretical and Computational Biophysics Department, Max-Planck-Institute for Biophysical Chemistry, Am Fassberg 11, 37077 Göttingen, Germany
*Present address: California Pacific Medical Center Research Institute, 475 Brannan St, San Francisco, CA 94107, USA
‡Author for correspondence (awodarz@gwdg.de)

Summary

Polarity of many cell types is controlled by a protein complex consisting of Bazooka/PAR-3 (Baz), PAR-6 and atypical protein kinase C (aPKC). In *Drosophila*, the Baz–PAR-6–aPKC complex is required for the control of cell polarity in the follicular epithelium, in ectodermal epithelia and neuroblasts. aPKC is the main signaling component of this complex that functions by phosphorylating downstream targets, while the PDZ domain proteins Baz and PAR-6 control the subcellular localization and kinase activity of aPKC. We compared the mutant phenotypes of an *aPKC* null allele with those of four novel *aPKC* alleles harboring point mutations that abolish the kinase activity or the binding of aPKC to PAR-6. We show that these point alleles retain full functionality in the control of follicle cell polarity, but produce strong loss-of-function phenotypes in embryonic epithelia and neuroblasts. Our data, combined with molecular dynamics simulations, show that the kinase activity of aPKC and its ability to bind PAR-6 are only required for a subset of its functions during development, revealing tissue-specific differences in the way that aPKC controls cell polarity.

Supplementary material available online at
http://jcs.biologists.org/cgi/content/full/122/20/3759/DC1

Key words: PAR complex, Asymmetric cell division, Cell polarity, Epithelial development

Introduction

Polarity is a universal feature of many different cell types, including epithelial cells, migrating cells and cells that divide asymmetrically, for instance the zygote of the nematode *C. elegans* or neural stem cells in *Drosophila* and vertebrates (Knust and Bossinger, 2002; Nelson, 2003; Wodarz and Huttner, 2003; Cowan and Hyman, 2004). Although these cell types are quite different in their function, shape and subcellular organization, the mechanisms that are involved in the establishment and maintenance of cell polarity have been conserved in evolution. One of the key regulators of cell polarity is the so-called PAR-3–PAR-6–aPKC complex, consisting of the PDZ (Postsynaptic density 95, Discs large, Zonula occludens 1) domain-containing proteins PAR-3 [also known as Bazooka (Baz) in *Drosophila*], PAR-6 and atypical protein kinase C (aPKC) (Wodarz, 2002; Suzuki and Ohno, 2006). This protein complex operates at the top of a functional hierarchy that in epithelia is responsible for the subdivision of the plasma membrane into an apical and a basolateral membrane domain and for the positioning of the zonula adherens (ZA), an adhesion belt encircling the apex of epithelial cells (Bilder et al., 2003; Johnson and Wodarz, 2003; Tanentzapf and Tepass, 2003; Hutterer et al., 2004; Harris and Peifer, 2005).

In *Drosophila*, the function of the PAR-3–PAR-6–aPKC complex in epithelial development has been studied in the embryonic ectoderm and in the somatic follicle epithelium of the ovary. The components of the PAR-3–PAR-6–aPKC complex are localized in the cortex underlying the apical plasma membrane and in the most apical region of the lateral cortex, overlapping with the subapical region (SAR) and the ZA (Wodarz et al., 2000; Petronczki and Knoblich, 2001; Harris and Peifer, 2005). Loss-of-function mutants for components of the PAR-3–PAR-6–aPKC complex show a loss of the apical plasma membrane domain, fail to assemble a ZA and lose the columnar structure typical of the wild-type embryonic ectoderm and the follicle epithelium (Müller and Wieschaus, 1996; Wodarz et al., 2000; Cox et al., 2001; Huynh et al., 2001; Petronczki and Knoblich, 2001; Rolls et al., 2003; Hutterer et al., 2004). The components of the complex are mutually dependent on each other for their correct subcellular localization, with the exception of Baz, for which the initial apical localization during cellularization is independent of the other complex members (Wodarz et al., 2000; Petronczki and Knoblich, 2001; Rolls et al., 2003; Hutterer et al., 2004; Harris and Peifer, 2005).

The PAR-3–PAR-6–aPKC complex is also required for setting up apical-basal polarity in neuroblasts (NBs), the stem cells of the central nervous system. Here, the complex localizes to the apical cortex and forms a crescent in pro- and metaphase (Kuchinke et al., 1998; Schober et al., 1999; Wodarz et al., 1999; Wodarz et al., 2000; Petronczki and Knoblich, 2001). The cell fate determinants Prospero, Brain Tumor (Brat) and Numb and their adapter proteins Miranda and Partner of Numb localize to the basal cortex of the NB and form crescents that do not overlap with the localization of the PAR-3–PAR-6–aPKC complex (Rhyu et al., 1994; Hirata et al.,

1995; Knoblich et al., 1995; Spana and Doe, 1995; Ikeshima-Kataoka et al., 1997; Shen et al., 1997; Lu et al., 1998; Schuldt et al., 1998; Bello et al., 2006; Betschinger et al., 2006; Lee et al., 2006b). In loss-of-function mutants for components of the PAR-3–PAR-6–aPKC complex, the cell fate determinants and their adapter proteins are mislocalized to the whole NB cortex and often fail to segregate correctly into the budding ganglion mother cell (GMC) (Schober et al., 1999; Wodarz et al., 1999; Petronczki and Knoblich, 2001; Rolls et al., 2003).

The PAR-3–PAR-6–aPKC complex also functions during the specification and polarization of the oocyte. In null mutants of *baz*, *par-6* and *aPKC*, an oocyte is initially specified, but the oocyte fate is not maintained in most egg chambers, resulting in the formation of 16 nurse cells and no oocyte (Cox et al., 2001; Huynh et al., 2001). At stages 9-10 of oogenesis, Baz and aPKC are required to localize PAR-1 and Staufen to the posterior oocyte cortex (Vaccari and Ephrussi, 2002; Benton and St Johnston, 2003; Tian and Deng, 2008).

How does the PAR-3–PAR-6–aPKC complex control cell polarity in these different cell types? According to genetic and biochemical data, mostly from *Drosophila* and mammalian tissue culture cells, Baz/PAR-3 is likely to function as a molecular scaffold that is required for the correct subcellular localization of the other components of the complex (Izumi et al., 1998; Schober et al., 1999; Wodarz et al., 1999; Joberty et al., 2000; Lin et al., 2000; Wodarz et al., 2000; Petronczki and Knoblich, 2001). PAR-6 functions as a molecular linker between cdc42 and aPKC and modulates the kinase activity of aPKC (Joberty et al., 2000; Johansson et al., 2000; Lin et al., 2000; Yamanaka et al., 2001; Peterson et al., 2004). The main active component of the complex is thought to be aPKC, which regulates the activities of other proteins functioning downstream in the cell polarity pathway by phosphorylation. Among the reported phosphorylation targets of aPKC that are involved in the regulation of cell polarity are Baz/PAR-3 (Nagai-Tamai et al., 2002), the transmembrane protein Crumbs (Crb) (Sotillos et al., 2004), Lethal giant larvae (Lgl) (Betschinger et al., 2003; Plant et al., 2003; Yamanaka et al., 2003), PAR-1 (Hurov et al., 2004; Kusakabe and Nishida, 2004; Suzuki et al., 2004) and Numb (Smith et al., 2007; Wirtz-Peitz et al., 2008).

Strong evidence for the importance of the kinase activity of aPKC for its function has been obtained both by overexpression of dominant negative and of constitutively active versions of aPKC in *Drosophila* (Betschinger et al., 2003; Sotillos et al., 2004; Lee et al., 2006a) and in mammalian tissue culture cells (Suzuki et al., 2001; Hurov et al., 2004; Smith et al., 2007). These studies have provided important insight into the function of aPKC in different contexts. However, these approaches relied on overexpression or ectopic expression of the respective modified forms of aPKC and do not necessarily reflect the requirement for the kinase activity of the endogenous protein expressed at physiological levels.

Here we present the molecular and phenotypic analysis of four new mutant alleles of *aPKC* in *Drosophila* that change single highly conserved amino acid residues. We show that these mutant forms of aPKC either fail to bind PAR-6 or lack kinase activity. Compared with the null allele *aPKC^k06403* used in all studies on *Drosophila* aPKC so far (Wodarz et al., 2000; Cox et al., 2001; Rolls et al., 2003; Harris and Peifer, 2007), the mutant phenotypes of the new alleles show pronounced tissue specificity with strong defects in some tissues and phenotypes indistinguishable from wild type in others. We propose that the functional requirement for aPKC is tissue specific and that both the binding to PAR-6 and the kinase activity of aPKC are only required for a subset of its functions.

Results

Isolation of four hypomorphic alleles of *aPKC*

In a genetic screen for EMS-induced mutations in maternally expressed genes that affect the patterning and integrity of the first instar larval epidermis, we isolated four mutations that showed cuticle phenotypes indicative of the loss of epithelial integrity reminiscent of mutations in the *crumbs* gene (Fig. 1) (Tepass et al., 1990; Luschnig et al., 2004). All four alleles were viable but female sterile in transheterozygous combinations with each other and with the *aPKC^k06403* mutation (Table 1) (Luschnig et al., 2004). *aPKC^k06403* has been classified as null allele because it is homozygous lethal and because no detectable protein is made in cells that are homozygous for this mutation (Wodarz et al., 2000; Rolls et al., 2003). Three of the four new *aPKC* alleles were homozygous viable, with the exception of *aPKC^psu417*, which is lethal at the second larval instar stage (Table 1) (Luschnig et al., 2004). In animals homozygous mutant for any of the four new *aPKC* alleles full-length mutant proteins were detectable by western blot (data not shown). These results together with the phenotypic and molecular analysis presented below show that all four mutations are hypomorphic alleles of *aPKC* that retain partial functionality.
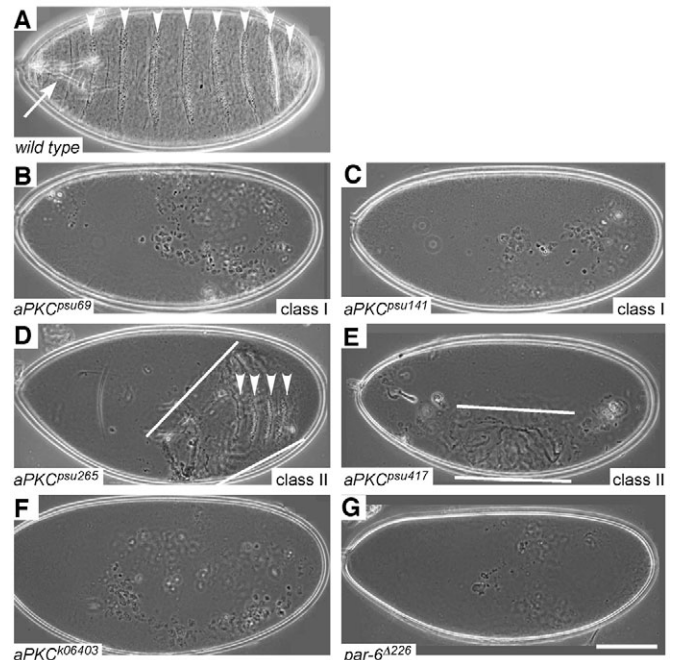

Fig. 1. *aPKC* mutant embryos derived from germ-line clones show loss of epithelial integrity in the epidermis. (A) Cuticle preparation of a wild-type embryo showing a contiguous cuticle with ventral denticle bands (arrowheads) and the head skeleton (arrow). (B-F) Cuticles of *aPKC* mutant embryos derived from germ-line clones show only crumbs of cuticle (B,C,F) or rudimentary patches of contiguous cuticle (D,E; between white lines), indicative of a breakdown of epithelial tissue structure. The phenotypes of the *aPKC^psu69* (B) and *aPKC^psu141* (C) class I alleles are indistinguishable from the null allele *aPKC^k06403* (F), whereas the phenotypes of the *aPKC^psu265* (D) and *aPKC^psu417* (E) class II alleles are much milder. Arrowheads in D point to rudimentary denticle bands. The cuticle phenotype of *par-6^Δ226* null mutant embryos derived from germ-line clones (G) resembles the *aPKC* null mutant phenotype. Anterior is to the left in all panels. Scale bar: 100 μm.

Table 1. Complementation analysis of *aPKC* alleles

	aPKC^psu69	aPKC^psu141	aPKC^psu265	aPKC^psu417	aPKC^k06403	Df Jp1
aPKC^psu69	++					
aPKC^psu141	++	++				
aPKC^psu265	o	++	o			
aPKC^psu417	o	+	o	−		
aPKC^k06403	+	+	o	o	−	
Df Jp1	−	o	−	−	−	−

++, Adult animals hatch in the expected Mendelian ratio; +, adult animals hatch in each experiment but numbers were less than expected from Mendels laws; o, occasional adult escapers hatched; −, no adult animals were observed.

Embryos derived from germ-line clones of the hypomorphic *aPKC* alleles loose apical-basal polarity in the embryonic ectoderm

Embryos homozygous mutant for the null allele *aPKC^k06403* develop normally because of maternally provided aPKC and die during larval stages when the maternal pool of aPKC is exhausted (Rolls et al., 2003). To analyze the phenotype of the new *aPKC* alleles during development of embryonic ectodermal epithelia in the absence of maternally provided wild-type aPKC, we generated germ-line clones of all four hypomorphic *aPKC* alleles, of the null allele *aPKC^k06403*, and of the null allele *par-6^Δ226*. Cuticle preparations of germ-line clone embryos from two hypomorphic *aPKC* alleles that we refer to as class I alleles (*aPKC^psu69* and *aPKC^psu141*) showed only scattered crumbs of cuticle (Fig. 1B,C), very similar to the
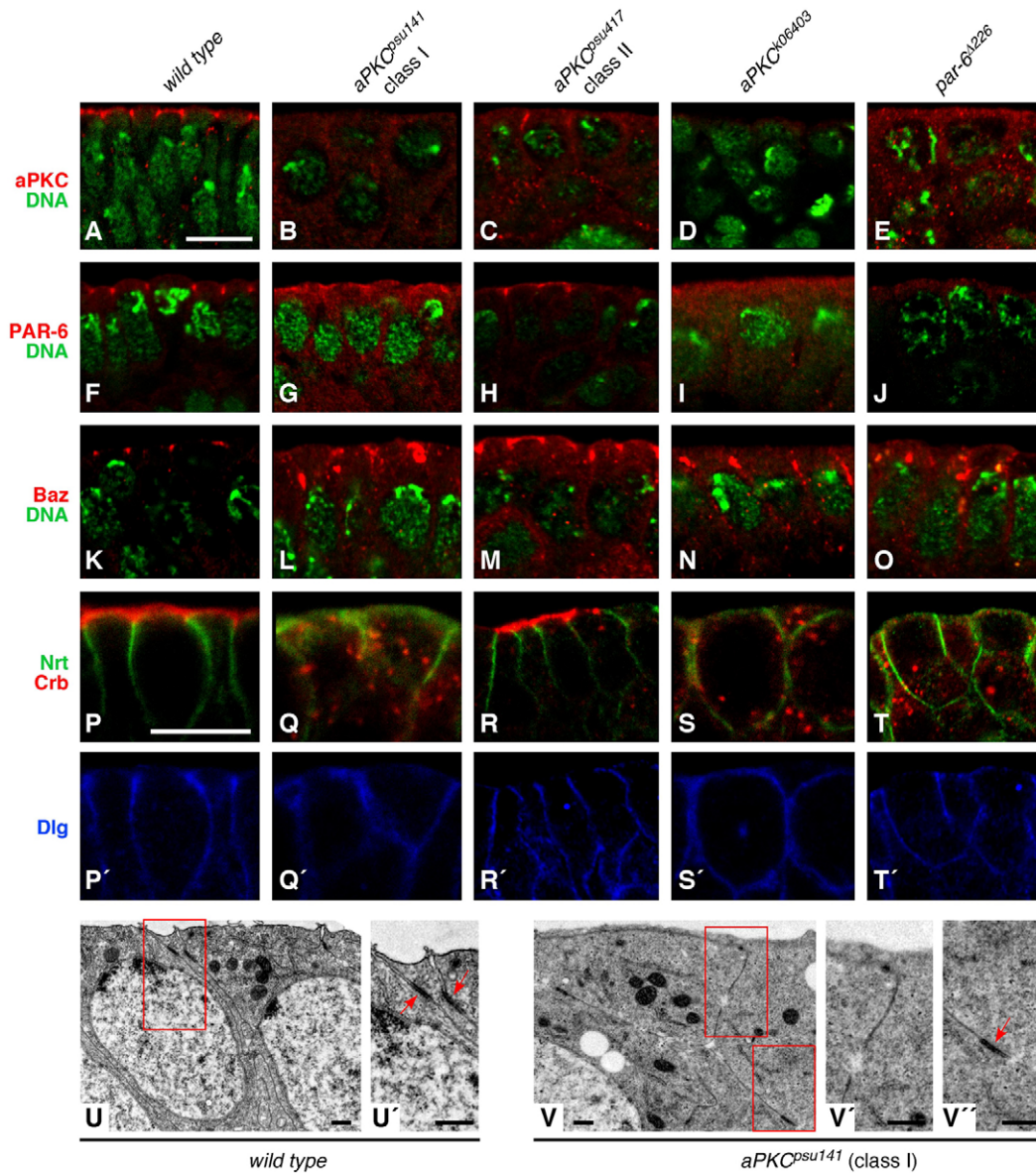

Fig. 2. Apical-basal polarity of the ectodermal epithelium is disrupted in *aPKC* and *par-6* mutant embryos derived from germ-line clones. The ectodermal epithelium of wild-type and mutant embryos at stage 7 was stained for aPKC (A-E), PAR-6 (F-J), Baz (K-O), Nrt, Crb and Dlg (P-T′). Scale bars: 10 μm (A-O); 10 μm (P-T). (U) Ultrastructure of the wild-type embryonic epidermis at stage 11. There is a contiguous electron dense ZA (U′, red arrows) in the apical portion of the lateral membrane. By contrast, *aPKC^psu141* mutant embryos at the same stage do not possess a contiguous ZA (V,V′). Instead, spot adherens junctions are found in ectopic positions along the lateral membrane (V″, arrow). Scale bars: 0.5 μm (U-V″). In all images apical is to the top.

cuticle phenotype of *aPKC^{k06403}* (Fig. 1F), *par-6* (Fig. 1G), *crb* and *sdt* mutants, which show complete disintegration of the embryonic epidermis (Tepass et al., 1990; Wodarz et al., 1995; Grawe et al., 1996; Bachmann et al., 2001; Hong et al., 2001; Petronczki and Knoblich, 2001; Hutterer et al., 2004; Harris and Peifer, 2005). The hypomorphic class II alleles (*aPKC^{psu265}* and *aPKC^{psu417}*) showed a weaker phenotype with contiguous patches of cuticle, including remnants of denticle belts (Fig. 1D,E).

In order to understand the development of this terminal phenotype in the *aPKC* germ-line clone embryos, we analyzed, by confocal microscopy, the subcellular localization of the mutant aPKC proteins and of several other proteins with a polarized localization in epithelia. Wild-type aPKC was localized to spots at the most apical region of the lateral plasma membrane of the ectodermal epithelium from cellularization onwards (Fig. 2A) (Wodarz et al., 2000; Harris and Peifer, 2005). By contrast, in embryos derived from germ-line clones, both mutant aPKC proteins encoded by the class I alleles were not localized to the cortex at all and instead showed a diffuse, cytoplasmic localization (Fig. 2B). aPKC proteins encoded by the class II alleles were localized similarly to wild-type aPKC at gastrulation (Fig. 2C) but became scattered along the lateral cortex later in development (data not shown). aPKC was diffusely localized in *par-6^{Δ226}* germ-line clone embryos lacking maternal and zygotic PAR-6, demonstrating that PAR-6 is required for cortical localization of aPKC (Fig. 2E).

In wild type, the subcellular localization of PAR-6 (Fig. 2F) is essentially identical to that of aPKC. PAR-6 was diffuse in the cytoplasm in embryos mutant for each of the class I *aPKC* alleles (Fig. 2G) and in embryos mutant for the null allele *aPKC^{k06403}* (Fig. 2I). In embryos mutant for the class II *aPKC* alleles, PAR-6 was localized to the apical cortex at gastrulation (Fig. 2H), as it was in the wild type.

The localization of Baz to the apical region of the lateral plasma membrane of the blastoderm epithelium at cellularization was unaffected by loss of *aPKC* function, both in germ-line clones of the null allele *aPKC^{k06403}* and in germ-line clones of all four hypomorphic alleles (data not shown) (Harris and Peifer, 2007). At this stage, Baz was also localized normally in *par-6^{Δ226}* mutant embryos (data not shown). During early gastrulation, the apicolateral localization of Baz was initially only slightly altered and Baz frequently formed larger particles in embryos mutant for all five *aPKC* alleles and in *par-6^{Δ226}* mutant embryos (Fig. 2K-O). During germ-band extension the apicolateral localization of Baz was gradually lost in embryos mutant for class I *aPKC* alleles, in embryos mutant for the null allele *aPKC^{k06403}*, and in *par-6^{Δ226}* mutant embryos (supplementary material Fig. S1) (Harris and Peifer, 2005; Harris and Peifer, 2007). In class II *aPKC* mutants, the localization of Baz at the corresponding developmental stages was heterogeneous, with areas showing almost normal localization and adjacent areas where Baz was completely mislocalized (supplementary material Fig. S1).

We also analyzed the subcellular localization of other proteins that show a polarized distribution in epithelia in *aPKC* mutant embryos. In wild-type epithelia, the transmembrane protein Crb localized to the subapical region (SAR) and to the free apical surface (Fig. 2P). Just below the SAR, DE-Cadherin (also known as Shotgun) localized to the zonula adherens (ZA; data not shown), and the transmembrane protein Neurotactin (Nrt) localized to the whole basolateral membrane (Fig. 2P). The cortical protein Discs large (Dlg) was present along the whole basolateral membrane and was enriched at the membrane

immediately basal to the ZA, at the position of the future septate junction (Fig. 2P′). In embryos mutant for class I *aPKC* alleles and in *aPKC^{k06403}* null mutant embryos, all four proteins were mislocalized (Fig. 2Q,S). Crb was completely lost from the SAR and from the apical membrane and was instead found in scattered vesicles in the cytoplasm (Fig. 2Q,S). DE-Cadherin, Nrt and Dlg were still present at the membrane but were not restricted to their normal position. Instead, all three proteins were detectable all around the cells, including the free apical membrane, pointing to a complete loss of plasma membrane polarity in the mutant embryos (Fig. 2Q,S). Moreover, the epithelial cells had lost their columnar, monolayered organization, rounded up and lost contact to each other (Fig. 2Q,S). *par-6^{Δ226}* mutant embryos showed the same phenotype with respect to the mislocalization of Crb, Nrt and Dlg (Fig. 2T). The mislocalization of the four polarity markers was less severe in class II *aPKC* mutant embryos, where patches of normal Crb localization to the apical membrane were still present (Fig. 2R).

Together, these results show that hypomorphic *aPKC* class I mutants show phenotypes similar to the *aPKC* and *PAR-6* null alleles with respect to cuticle phenotype and the subcellular localization of several polarity markers, whereas *aPKC* class II alleles produced weaker phenotypes in every aspect that we analyzed.

Ultrastructural examination of *aPKC^{psu141}* (class I) mutant embryos revealed that the neuroectodermal epithelium did not possess a contiguous ZA, consistent with the observed mislocalization of DE-cadherin (Fig. 2V). Instead, spot adherens junctions were found in ectopic positions along the lateral plasma membrane (Fig. 2V).

Mutations in *crb*, *sdt* and several other genes that result in loss of epithelial cell polarity and failure to form a ZA cause massive apoptosis in epithelial cells from mid-embryogenesis onwards (Tepass and Knust, 1993; Grawe et al., 1996). This was also the case for the four hypomorphic *aPKC* alleles, as detected by TUNEL and staining for the activated caspase Drice (supplementary material Fig. S2B). Apoptotic cells frequently were not internalized and engulfed by macrophages, as in wild type (supplementary material Fig. S2C) but remained on the surface of the embryo (supplementary material Fig. S2D).

aPKC is required for the correct localization of PAR-6 and Miranda in embryonic neuroblasts

In wild-type NBs at metaphase, aPKC, PAR-6 and Baz colocalize in an apical cortical crescent whereas Miranda forms a basal cortical crescent (Fig. 3A,H,O). In order to study the requirement for *aPKC* during the asymmetric division of embryonic neuroblasts, we analyzed germ-line clone embryos by confocal microscopy. The mutant aPKC proteins encoded by the class I alleles were localized diffusely in the cytoplasm and never formed apical crescents (Fig. 3B,C; supplementary material Table S1). Complete mislocalization of aPKC to the cytoplasm was also observed in *par-6^{Δ226}* mutant embryos (Fig. 3G). By contrast, the mutant aPKC proteins encoded by the class II alleles localized to the apical cortex of neuroblasts in 78% and 53% of cases, respectively (Fig. 3D,E; supplementary material Table S1).

PAR-6 never formed apical crescents in NBs of *aPKC^{k06403}* null mutant embryos (Fig. 3M) and in only 29% of germ-line clone *aPKC^{psu69}* mutant embryos (Fig. 3I). In embryos mutant for the other three hypomorphic alleles the apical localization of PAR-6 in NBs was also reduced, but not to the same extent as in the null and *aPKC^{psu69}* mutants (Fig. 3J-L; supplementary material Table S2).
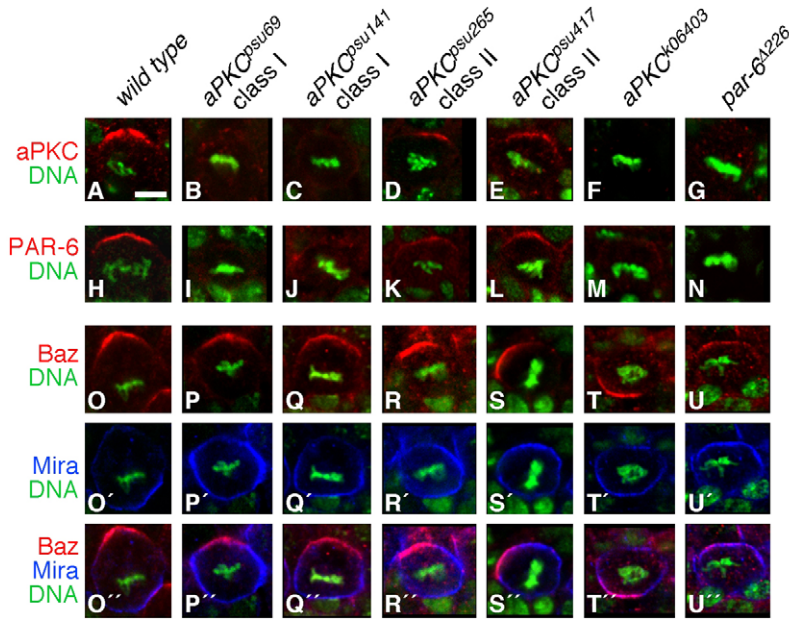
Fig. 3. Neuroblast polarity in *aPKC* and *par-6* mutant embryos derived from germ-line clones. Wild-type and mutant NBs at metaphase were stained for aPKC (red; A-G), PAR-6 (red; H-N), Baz (red) and Mira (blue; O-U″). DNA was stained with YOYO-1 (green). Note that spindle orientation deduced from the orientation of the metaphase plate and the position of the Baz crescent was occasionally abnormal (S,T). Scale bar: 5 μm. In all panels, apical is up.

The apical localization of Baz in NBs was only slightly affected in germ-line clone embryos of all four hypomorphic *aPKC* alleles (Fig. 3P-S; supplementary material Table S3). Only in *aPKC^{k06403}* null mutant embryos was apical localization of Baz reduced to 30% (Fig. 3T; supplementary material Table S3). In *par-6^{Δ226}* mutant embryos, Baz was still localized to the apical cortex of NBs in 67% of the embryos (Fig. 3U).

The PAR-3–PAR-6–aPKC complex is required for the basal localization of cell fate determinants in metaphase NBs (Schober et al., 1999; Wodarz et al., 1999; Petronczki and Knoblich, 2001; Rolls et al., 2003). In NBs of *aPKC^{k06403}* null mutant embryos the adapter protein Miranda never localized as a basal crescent as in wild type but instead was found all around the cortex, at the apical cortex or diffuse in the cytoplasm (Fig. 3T; supplementary material Table S4). The four hypomorphic *aPKC* alleles resulted in Mira being either localized to the basal cortex or to the whole cortex to different degrees, with the weakest defects seen in the *aPKC^{psu265}* class II mutants and the strongest defects seen in the *aPKC^{psu417}* class II mutants (Fig. 3P-S; supplementary material Table S4).

We noted that the orientation of the metaphase plate and of the asymmetric crescent of Baz was abnormal in a fraction of *aPKC* mutant NBs in embryos derived from germ-line clones (Fig. 3S,T). The quantification of these defects is shown in supplementary material Fig. S3.

Female sterility in animals mutant for the hypomorphic *aPKC* alleles

Females homozygous for any of the three viable hypomorphic alleles were sterile and their ovaries lost the monolayered organization of the follicle epithelium (Fig. 4B). In follicle cells that were in contact with germ-line cells PAR-6 was apically localized (Fig. 4B), similar to wild-type follicle cells (Fig. 4A). By contrast, follicle cells that did not touch germ-line cells because of the multilayering of the epithelium showed diffuse cortical staining for PAR-6 (Fig. 4B). In many mutant egg chambers, the follicle epithelium was discontinuous and failed to ensheath the germ-line cells (Fig. 4B). In all transheterozygous combinations of the hypomorphic *aPKC* alleles the females were sterile and

showed the same defects as observed in homozygous mutant females.

Follicle cell polarity is normal in clones of cells homozygous for hypomorphic *aPKC* alleles

To analyze the effect of the mutations in the new *aPKC* alleles on the integrity and polarity of the follicle epithelium, we generated follicle cell clones. Although follicle cell clones of the null allele *aPKC^{k06403}* showed a complete loss of apical-basal polarity and extensive multilayering of the mutant cells (Fig. 4E) (Cox et al., 2001; Abdelilah-Seyfried et al., 2003), clones of each of the new *aPKC* alleles showed only subtle defects, if any (Fig. 4C,D). In general, follicle cells mutant for any of the hypomorphic *aPKC* alleles showed normal apical-basal polarity with respect to the subcellular localization of the mutant aPKC itself and of the apical markers Baz, PAR-6 and Crb (Fig. 4C,D; and data not shown). In rare cases we observed egg chambers with follicle cell clones that had gaps in the follicle epithelium (Fig. 4D).

Oocyte determination and polarity are unaffected in germ-line clones of the hypomorphic *aPKC* alleles

To investigate the functionality of the proteins encoded by the four new *aPKC* alleles in germ-line cells of the ovary without compromising aPKC function in the follicle epithelium, we generated clones of homozygous mutant germ-line cells by FLP-FRT-mediated mitotic recombination. Oocyte determination occured normally in the vast majority of egg chambers with germ-line clones (93.7%, *n*=111), as demonstrated by expression of the oocyte-specific Orb protein in only one of the 16 germ-line cells after stage 4 of oogenesis (Fig. 4F,G). By contrast, in only 28% (*n*=64) of germ-line clones of the null allele *aPKC^{k06403}*, was an oocyte specified (Fig. 4H), consistent with published data (Cox et al., 2001). The germ-line clone oocytes mutant for any of the four new alleles did not show any obvious defects in the localization of Staufen, Gurken (Fig. 4J,K; 100% normal localization of both proteins, *n*=49) and Vasa (data not shown) at stage 9-10, indicating that the anterior-posterior polarization of the oocyte was unaffected. The localization of Staufen and Gurken in *aPKC^{k06403}* mutant
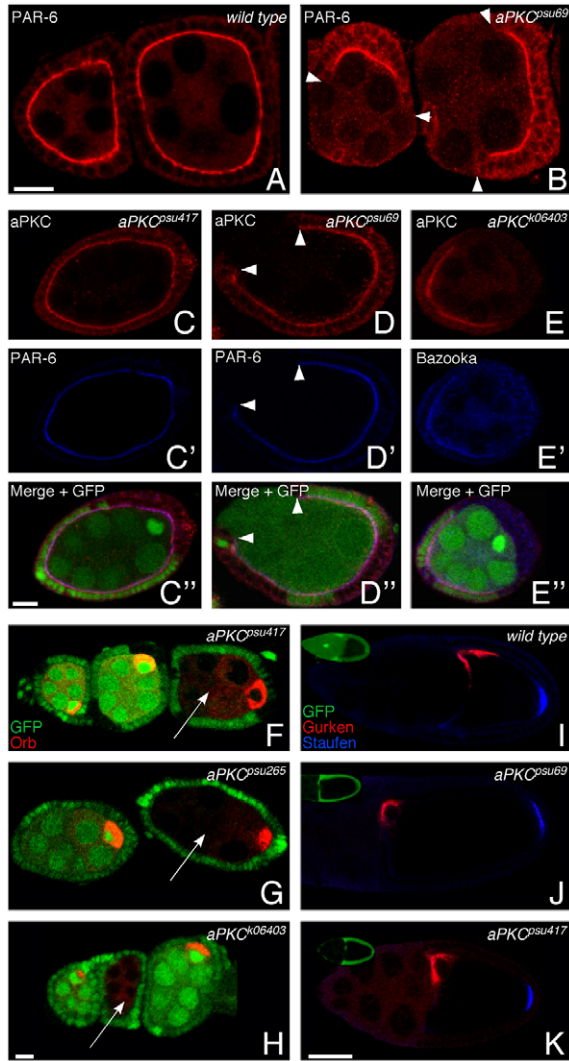
Fig. 4. *aPKC* mutant phenotypes in oogenesis. (A) In wild-type egg chambers, the follicular epithelium has a regular, monolayered structure and PAR-6 is localized to the apical cortex of the follicle cells. (B) Egg chambers of homozygous *aPKC^psu69* mutant females show both multilayering and large gaps (arrowheads) in the follicle epithelium. Note that PAR-6 is still localized apically in follicle cells that are in direct contact with the germ-line cells. Scale bar: 10 μm (A,B). (C-E′) The phenotype of the hypomorphic *aPKC* alleles in homozygous mutant follicle cell clones is much milder than that of the *aPKC* null allele. Follicle cell clones of *aPKC^psu417* (C,C′) and of *aPKC^psu69* (D,D′) show a normal monolayered tissue structure and correct localization of the mutant aPKC (red) and PAR-6 (blue) to the apical cortex. Occasionally, gaps are observed in the follicle epithelium of egg chambers carrying clones of *aPKC* mutant cells (D,D′,D″, arrowheads). In contrast to the hypomorphic *aPKC* alleles, follicle cell clones of the null allele *aPKC^k06403* (E,E′,E″) show multilayering of the epithelium and a complete loss of the apical localization of Bazooka (blue). Clones of homozygous mutant follicle cells are marked by the absence of GFP (green). Scale bar: 10 μm (C-E″). (F-H) Oocyte determination occurs normally in *aPKC^psu417* (F) and *aPKC^psu265* (G) germ-line clones, but not in the the null allele *aPKC^k06403* germ-line clone (H), which shows loss of the oocyte in most egg chambers. Oocytes are marked by staining for Orb (red) and homozygous mutant cells are marked by absence of GFP (green, arrows). Scale bar: 10 μm (F-H). (I-K) Anterior-posterior polarity of the oocyte is normal in *aPKC^psu69* and *aPKC^psu417* germ-line clones. In wild-type oocytes (I), Gurken (red) is localized to the anterior dorsal cortex and Staufen (blue) to the posterior cortex of the oocyte. The localization of Gurken and Staufen in germ-line clones of *aPKC^psu69* (J) and *aPKC^psu417* (K) is indistinguishable from that in wild-type. Germ-line clones are marked by absence of GFP staining (insets) in nurse cells and oocytes. Scale bar: 50 μm (I-K). Anterior is to the left in all panels.

oocytes at stage 9-10 was also normal in most cases (95% normal localization, *n*=20; data not shown), suggesting that aPKC has only a minor function in the control of anterior-posterior oocyte polarity in late oogenesis.

The four hypomorphic *aPKC* alleles encode mutant proteins with changes in single, highly conserved amino acid residues
Sequencing of genomic DNA from the *aPKC* locus of the mutant chromosomes revealed the presence of point mutations leading to single amino acid changes in all four alleles (Fig. 5A). All four mutations alter amino acid residues that are identical in the aPKCs of all species analyzed so far, indicating that these residues are functionally important (supplementary material Fig. S4).

The position of the altered amino acids resulting from the four novel alleles allowed predictions regarding the functions that may be affected by the mutations. The mutation in *aPKC^psu69* changes cysteine 122 to tyrosine (Fig. 5A; supplementary material Fig. S4). Since this residue is positioned close to the PB1 domain that is required for binding of aPKC to PAR-6 (Noda et al., 2003; Wilson et al., 2003; Hirano et al., 2005), we tested whether the binding to PAR-6 was affected in this mutant protein. To that aim, we expressed N-terminally GFP-tagged versions of full-length wild-type aPKC and the four mutant versions of aPKC in *Drosophila* S2 cells and checked for binding to the endogenous PAR-6 by coimmunoprecipitation experiments. Whereas GFP-wtaPKC, GFP-aPKC^psu141^, GFP-aPKC^psu265^ and GFP-aPKC^psu417^ all bound endogenous PAR-6, the binding of GFP-aPKC^psu69^ to PAR-6 was completely abolished, irrespective of whether the anti-PAR-6 antibody or the anti-GFP antibody was used for coimmunoprecipitation (Fig. 5B). By contrast, both GFP-wtaPKC and all four mutant versions of GFP-aPKC bound equally well to Lgl and to Baz (data not shown), two additional known binding partners of aPKC (Wodarz et al., 2000; Betschinger et al., 2003).

The mutation in *aPKC^psu141* changes phenylalanine 423 to isoleucine (Fig. 5A). This residue is located within the activation loop of the kinase and lies right next to threonine 422, which is the predicted phosphorylation target of phosphatidylinositol dependent kinase 1 (PDK1; supplementary material Fig. S4) (Chou et al., 1998; Le Good et al., 1998). Since phosphorylation of T422 is sequence specific, we predicted that mutation of F423 prevents phosphorylation of T422 by PDK1 and thus blocks activation of aPKC. A phosphospecific antibody is available that distinguishes aPKC phosphorylated at T422 from the unphosphorylated form. In S2 cells transfected with wild-type GFP-aPKC, the GFP-tagged protein was recognized by the phosphospecific antibody, in contrast to the mutant GFP-aPKC^psu141^ (Fig. 5C). In extracts of heads of flies homozygous for *aPKC^psu141*, we could not detect any endogenous mutant aPKC protein with the antibody specific for aPKC phosphorylated at T422 (Fig. 5C).

The mutation in *aPKC^psu265* changes the conserved alanine residue A291 to valine (Fig. 5A). A291 lies in the immediate vicinity of K293 (supplementary material Fig. S4), a lysine residue in the ATP binding pocket of the kinase domain that is essential for the kinase activity of all aPKC familiy members (Newton, 1995). The mutation in *aPKC^psu417* changes the conserved glycine residue G347 in the kinase domain to an asparagine residue (Fig. 5A). To test whether any of the four mutations described here affect the kinase activity of the mutant proteins, we performed in vitro kinase assays, and for comparison included the mutant protein GFP-aPKC^K293A^, which carrries a point mutation leading to the exchange of the active site lysine residue for alanine which renders it kinase-dead (Sotillos
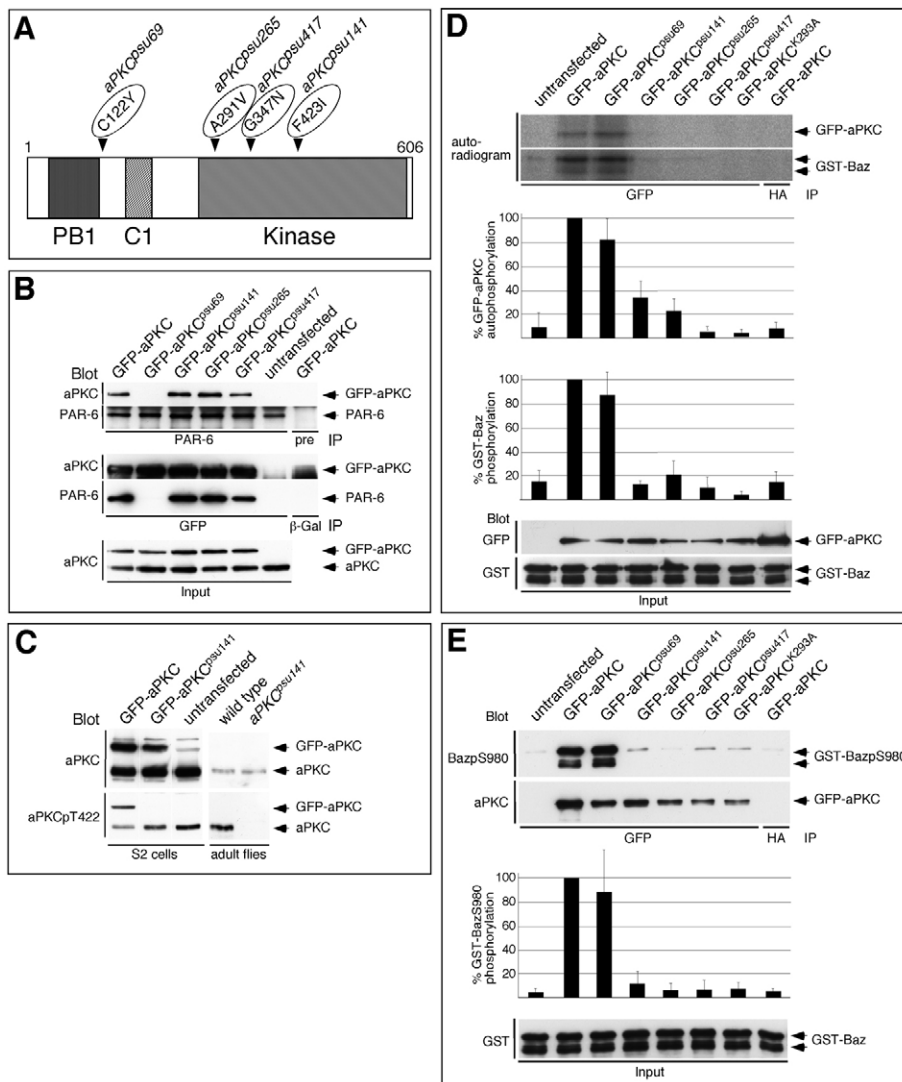
Fig. 5. Biochemical properties of mutant aPKC proteins. (A) Structure of the aPKC protein. The position of the mutations in the four new *aPKC* alleles is indicated by arrowheads. (B) The GFP-aPKC[psu69] protein does not bind to PAR-6. S2 cells were transfected with wild-type GFP-aPKC and with the four mutant versions of GFP-aPKC. Untransfected S2 cells were used as negative control. The cell lysates were subjected to immunoprecipitation (IP) followed by western blotting (Blot) with the indicated antibodies. Preimmune serum (pre; for PAR-6 IPs) or anti-β-galactosidase antibodies (β-Gal; for GFP IPs) were used as negative controls. (C) The mutant aPKC[psu141] protein is not recognized by the phospho-specific antibody directed against the phosphorylated threonine residue T422. Lysates from S2 cells transfected with GFP-aPKC or with GFPaPKC[psu141] were subjected to western blotting with either an antibody that recognizes aPKC irrespective of its phosphorylation state (aPKC) or with an antibody that specifically recognizes aPKC phosphorylated at T422 (aPKCpT422). A T422 phospho-specific band corresponding to GFPaPKC, but not to GFPaPKC[psu141] was detected. Untransfected S2 cells were used as loading control. This observation was confirmed in western blots of adult head extracts of wild-type and *aPKC[psu141]* homozygous mutant flies (right). (D) Three of the four mutant aPKC proteins show strongly reduced kinase activity. In vitro kinase assays using [γ-^{32}P]ATP were performed on anti-GFP immunoprecipitates of lysates of S2 cells transfected with either wild-type GFP-aPKC, with any of the four mutant GFP-aPKC versions and with GFP-tagged kinase-dead aPKC (GFP-aPKC[K293A]). Untransfected cells and cells transfected with wild-type GFP-aPKC but immunoprecipitated with anti-HA antibody were used as negative controls. Both autophosphorylation of GFP-aPKC and phosphorylation of a GST-Baz fusion protein containing the aPKC target site S980 were measured by autoradiography. One representative autoradiogram is shown. The quantitative analysis of four independent in vitro kinase assays is shown in the bar diagrams below the autoradiographs. Values are percentage phosphorylation relative to that of the wild-type GFP-aPKC protein. The input for the kinase assay (top) is shown at the bottom. (E) Three of the four mutant aPKC proteins are kinase-dead with respect to phosphorylation of S980 of Baz. In vitro kinase assays were performed with non-radioactive ATP as phosphate donor and phosphorylation of the GST-Baz fusion protein was detected in western blots using a phospho-specific antibody against S980 of Baz. The immunoprecipitated GFP-aPKC from the same experiment was also detected by western blotting. Quantification of the blots with the phospho-specific Baz antibody from four independent experiments and the GST-Baz input corresponding to the kinase assay (top) are shown at the bottom.

et al., 2004). The full-length wild-type GFP-aPKC fusion protein and the GFP-aPKC[psu69] fusion protein showed comparable levels of kinase activity when tested for autophosphorylation or phosphorylation of a GST-Baz fusion protein containing the aPKC target site S980 in radioactive in vitro kinase assays (Fig. 5D). By

contrast, the mutant fusion proteins GFP-aPKC[psu141], GFP-aPKC[psu265] and GFP-aPKC[psu417] showed strongly reduced kinase activity in both assays with GFP-aPKC[psu417], being indistinguishable in its activity from the kinase-dead mutant GFP-aPKC[K293A] (Fig. 5D). To further consolidate this finding, we performed in vitro kinase
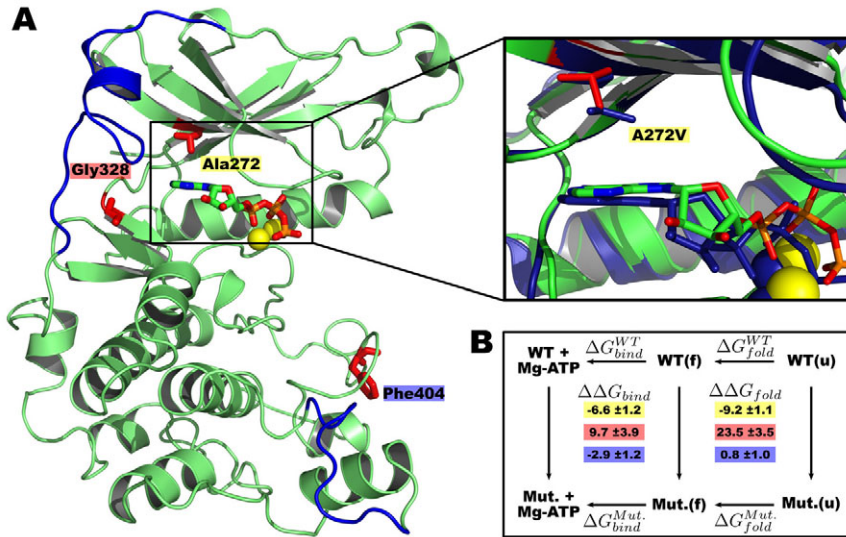
Fig. 6. Structure of human PKCɩ and thermodynamic cycles. (A) Overall structure of human PKCɩ with modeled structure elements (blue) and mutated residues (red). The enlarged view (right) compares the ATP binding pocket of the wild-type structure (green) with that of the A272V mutant (dark blue). (B) Thermodynamic cycles used in the free energy calculations described in the text. WT and Mut. refer to the wild-type and each of the considered mutant structures, respectively; the indices (f) and (u) refer to the folded and unfolded states, respectively. The color codings of the free energy double differences ($\Delta\Delta G_{bind}$ and $\Delta\Delta G_{fold}$) correspond to the respective mutated amino acids in A.

assays using a phosphospecific antibody directed against pS980 of Baz (Krahn et al., 2009), which is homologous to pS827 of mammalian PAR-3 (Nagai-Tamai et al., 2002). This highly substrate-specific assay confirmed the findings from the radioactive kinase assays and showed that GFP-aPKC^{psu141} and GFP-aPKC^{psu265} also have little if any kinase activity in vitro (Fig. 5E).

Effects of the mutations on ATP binding and protein folding

To test if the observed loss of kinase function for the point mutations A291V (aPKC^{psu265}), G347N (aPKC^{psu417}) and F423I (aPKC^{psu141}) is either due to changed substrate affinity or, alternatively, to a possible destabilization of the folded state, free energy calculations based on extended molecular dynamics simulations were carried out. Since the crystal structure of *Drosophila* aPKC has not been solved, we used the published structure of human PKCɩ (Messerschmidt et al., 2005) (Fig. 6) as the basis for our calculations, which is 67% identical to *Drosophila* aPKC. All three residues affected by the mutations in *Drosophila* aPKC are identical to the homologous residues in human PKCɩ (supplementary material Fig. S4). Moreover, the regions harboring the three mutations are highly conserved in both proteins, such that the relevant free energy double differences are expected to be unaffected by distant sequence differences. A similar argument holds for the structural elements (Fig. 6A, blue), which were not resolved in the crystal structure and, therefore, had to be modeled. Table 2 shows the relevant differences as well as the double differences $\Delta\Delta G_{fold(3/5)}$ and $\Delta\Delta G_{bind}$. The latter express the change in folding free energy and ATP binding free energy, respectively, caused by the mutation. Our free energy calculations predict a 14 times lower ATP binding affinity for the A272V mutation (homologous to *Drosophila* A291V) as compared with the wild type, which provides

a plausible explanation for the observed loss of function. The ATP binding affinity of the G328N mutation (homologous to *Drosophila* G347N), in contrast, is higher by a factor of 50 and, therefore, loss of function of that mutant probably has other causes. Because in this case the folding equilibrium constant is larger by four orders of magnitude, we suggest misfolding as the most likely alternative explanation. For the F404I mutant (homologous to *Drosophila* F423I), both the ATP binding affinity as well as the folding free energy are nearly unchanged, thus ruling out both of these possible explanations. Also, this residue is unlikely to affect the ATP binding affinity of *aPKC* because of the large distance between F404 and the ATP-binding pocket (Fig. 6A).

Discussion

aPKC is often regarded as the main catalytically active component of the PAR-3–PAR-6–aPKC complex that controls cell polarity by phosphorylation of critical targets. In this model, the other two components of the complex, Baz/PAR-3 and PAR-6 serve mainly as scaffolding proteins that are responsible for the correct localization of aPKC and for regulating its catalytic activity (Wodarz, 2005; Suzuki and Ohno, 2006; Knoblich, 2008). However, this concept has never been rigorously tested because of the lack of mutations in *aPKC* that specifically compromise the binding of aPKC to PAR-6 or its kinase activity but leave the remainder of the protein intact. All genetic analyses performed in *Drosophila* so far relied on the *aPKC^{k06403}* null allele, which does not give rise to any detectable aPKC protein (Wodarz et al., 2000; Cox et al., 2001; Rolls et al., 2003). Here we have analyzed four new alleles of *aPKC* carrying single base changes leading to the exchange of single highly conserved amino acid residues. The molecular and biochemical analysis of these alleles revealed that

Table 2. Calculated free energy differences between wild-type protein and the three mutant proteins

Mutant	ΔG_f	ΔG_{+ATP}	ΔG_{u3}	ΔG_{u5}	$\Delta\Delta G_{bind}$	$\Delta\Delta G_{fold(3)}$	$\Delta\Delta G_{fold(5)}$
A272V	−101.4±1.0	−94.8±0.7	−91.9±0.4	−93.2±0.4	−6.6±1.2	−9.6±1.0	−8.2±1.0
G328N	−337.5±3.4	−347.1±1.9	−357.6±0.7	−361.0±0.8	9.7±3.9	20.1±3.5	23.5±3.5
F404I	9.8±0.8	12.8±0.9	12.9±0.5	9.0±0.6	−2.9±1.2	−3.1±0.9	0.8±1.0

ΔG_f denotes the free energy difference for the folded and ligand-free protein, ΔG_{+ATP} for the Mg^{2+}-ATP bound complex, ΔG_{u3} for the tripeptide, and ΔG_{u5} for the pentapeptide. $\Delta\Delta G_{bind}=\Delta G_f−\Delta G_{+ATP}$ denotes the ATP binding free energy difference between wild type and the respective mutant, $\Delta\Delta G_{fold(3)}$ between ΔG_f and ΔG_{u3}, and $\Delta\Delta G_{fold(5)}$ between ΔG_f and ΔG_{u5}. All energies are given in kJ/mol.

either the binding to PAR-6 or the kinase activity of aPKC is abolished in the mutant proteins. Our free energy calculations of the three mutants lacking kinase activity suggest that in one mutant the binding of ATP is strongly compromised while in a second mutant protein misfolding is the most likely cause for the observed loss of function. Both the binding to PAR-6 and the kinase activity were thought to be essential for the correct localization and function of aPKC, according to the model discussed above. Nonetheless, all four alleles behave as hypomorphs by genetic criteria and with regard to the severity of the mutant phenotypes. Interestingly, the severity of the mutant phenotype differs dramatically between different tissues. All four hypomorphic alleles result in severe defects in the embryonic epidermis and in embryonic neuroblasts, while oocyte determination and the polarity of the follicle epithelium are largely unaffected.

The four hypomorphic alleles of *aPKC* result in strong mutant phenotypes in embryonic epithelia

Embryos derived from germ-line clones for any of the four hypomorphic *aPKC* alleles showed severe defects in ectodermal epithelia. Their cuticle phenotypes, in particular those of the class I alleles, were very similar to those of *crb*, *sdt*, *baz* and *par-6* mutants, which have almost complete loss of apical-basal polarity and integrity of ectodermal epithelia (Tepass et al., 1990; Grawe et al., 1996; Müller and Wieschaus, 1996; Tepass, 1996; Bachmann et al., 2001; Hong et al., 2001; Petronczki and Knoblich, 2001). This was confirmed at the ultrastructural level, since the defects in ZA formation in *aPKC* mutant embryos were very similar to those of *crb*, *sdt* and *baz* mutants (Grawe et al., 1996; Müller and Wieschaus, 1996; Tepass, 1996; Bachmann et al., 2001; Hong et al., 2001). Consistent with these observations, Crb was not localized to the plasma membrane at all and instead was in cytoplasmic vesicles in class I *aPKC* mutant embryos. It is conceivable that the trafficking of Crb to the apical plasma membrane is dependent on direct phosphorylation by aPKC (Sotillos et al., 2004). Alternatively, because Crb and its binding partner Sdt/PALS1 can directly bind to PAR-6 (Hurd et al., 2003; Lemmers et al., 2004; Wang et al., 2004; Kempkens et al., 2006) and aPKC and PAR-6 are mutually dependent on each other for their correct localization in the epidermis, the mislocalization of Crb in *aPKC* mutant embryos could also be caused by the mislocalization of PAR-6. It has recently been reported that Cdc42 and the PAR-3–PAR-6–aPKC complex are required to suppress apical endocytosis in tissues undergoing strong morphogenetic movements, such as the neurogenic ectoderm (Harris and Tepass, 2008). Our finding that in *aPKC* mutant embryos Crb is in vesicles instead of being localized to the apical plasma membrane is fully consistent with this model.

The severity of the mutant phenotypes in the epidermis differed considerably between class I and class II alleles. This difference cannot be accounted for by a difference in the kinase activity of the mutants, since both proteins encoded by the class II alleles and the protein encoded by the class I allele *aPKC^psu141* showed the same reduction in kinase activity, which was indistinguishable from the kinase-dead aPKC^K293A protein. We therefore speculate that the difference may be caused by the effects of the mutations on the scaffolding function of aPKC. The protein encoded by the class I allele *aPKC^psu69* is unable to bind PAR-6 and thus cannot assemble a functional PAR-3–PAR-6–aPKC complex. Similarly, the protein encoded by the class I allele *aPKC^psu141* carries a mutation in the recognition sequence for PDK1 and thus may fail to bind PDK1. Moreover, the failure of the aPKC^psu141 protein to be phosphorylated

by PDK1 may prevent a conformational change that allows additional proteins to bind aPKC (Hirai and Chida, 2003).

Quite surprisingly, the class II allele *aPKC^psu417* is the only one of the four hypomorphic aPKC alleles that is lethal in homozygosity. Since it is viable in combination with all other alleles, including the null allele *aPKC^k06403*, we believe that the lethality of this allele is caused by a second site hit and not by the loss of aPKC function.

Binding to PAR-6 and kinase activity of aPKC are dispensable for the function of aPKC in the follicle epithelium

In the follicle epithelium, even in large clones of follicle cells mutant for any of the four hypomorphic alleles the localization of the mutant aPKC itself, PAR-6 and Baz was normal. Also, the mutant follicle cells were always organized in a monolayer. By contrast, follicle cell clones with the null allele *aPKC^k06403* showed severe defects. *aPKC^k06403* mutant cells completely lost polarity, failed to localize PAR-6 and Baz to the apical cortex and piled up on top of each other. Thus, although the presence of aPKC is essential, neither the binding between aPKC and PAR-6 nor the kinase activity of aPKC is required for normal development of the follicle epithelium during oogenesis.

All females homozygous mutant for any of the three viable *aPKC* alleles showed multilayering of the follicle epithelium, whereas follicle cell clones of the same alleles never showed this phenotype. Nonetheless, even in areas with multilayered tissue organization, follicle cells that were in contact with germ-line cells showed normal apical-basal polarity. Thus, we favor the idea that in ovaries of animals homozygous mutant for one of the hypomorphic *aPKC* alleles the simultaneous loss of aPKC function in germ-line cells and follicle cells may disturb the interaction between these cell types early during egg chamber formation, which could cause the multilayering of the follicle epithelium.

Why are the mutant phenotypes of the four hypomorphic *aPKC* alleles much stronger in the embryonic ectodermal epithelium than in the adult follicle epithelium? This is not the case for the null allele of *aPKC*, which causes an almost complete loss of cell polarity and tissue integrity in both tissues. The reason may lie in the different ways these two epithelia are formed. The polarity of the embryonic ectodermal epithelium is established at cellularization, when no basement membrane is present, and thus relies predominantly on apical cues, in particular the PAR-3–PAR-6–aPKC complex and the Crb-Sdt complex (Tepass et al., 1990; Wodarz et al., 1995; Müller and Wieschaus, 1996; Bachmann et al., 2001; Hong et al., 2001; Harris and Peifer, 2004). By contrast, the establishment of polarity in the follicle epithelium relies predominantly on basal cues provided by the basement membrane and only later on apical and lateral cues provided by the contact with germ-line cells and adjacent epithelial cells (Tanentzapf et al., 2000; Schneider et al., 2006; Mirouse et al., 2009).

aPKC function in embryonic neuroblasts

Regarding their subcellular localization in embryonic NBs, the mutant proteins encoded by the four hypomorphic *aPKC* alleles behaved as they do in the epidermis: the mutant proteins encoded by the class I alleles never formed apical crescents in NBs, whereas the proteins encoded by the class II alleles were localized to the apical cortex in the majority of NBs. Similarly, apical localization of PAR-6 was abolished in the majority of NBs mutant for class I *aPKC* alleles but was largely normal in class II mutant NBs. Vice versa, aPKC was completely mislocalized in NBs mutant for *par-6*. Thus, we conclude that aPKC and PAR-6 are codependent for

their proper localization in NBs, but that the kinase activity of aPKC is not essential in this context.

In contrast to the mislocalization of aPKC and PAR-6 in the hypomorphic *aPKC* mutant NBs, the localization of Baz was normal in most cases. However, only 30% of NBs mutant for the null allele *aPKC^{k06403}* showed apical localization of Baz. This finding suggests that neither the binding between aPKC and PAR-6 nor the kinase activity of aPKC is required for the apical localization of Baz in NBs, as long as aPKC is available as a binding partner of Baz. Support for this interpretation comes from our finding that the mutant proteins encoded by all four hypomorphic *aPKC* alleles retain their ability to bind Baz. An earlier study reported that apical localization of Baz in larval NBs was independent of aPKC (Rolls et al., 2003). This result could reflect a different requirement for aPKC function in embryonic and larval NBs. Alternatively, residual maternal aPKC protein still present in larval NBs could explain this apparent discrepancy.

The PAR-3–PAR-6–aPKC complex is required for the localization of cell fate determinants, including Prospero and Numb, to the basal NB cortex (Wodarz, 2005; Knoblich, 2008). This function is mediated by the activity of aPKC which phosphorylates Lgl in the apical cortex and thus prevents its association with the cortical cytoskeleton (Betschinger et al., 2003; Plant et al., 2003; Yamanaka et al., 2003; Betschinger et al., 2005). Cortical Lgl in turn is required for the cortical localization of the adapter protein Miranda, which recruits Prospero to the cortex. In embryos mutant for any of the four hypomorphic *aPKC* alleles Miranda was mislocalized in metaphase NBs, but not to the same extent and with the same penetrance as in embryos mutant for the null allele *aPKC^{k06403}*. These findings show that the kinase activity of aPKC is important but may not be absolutely essential for inactivation of Lgl.

The four hypomorphic alleles of *aPKC* are fully functional in oocyte determination

The hypomorphic nature of the four new *aPKC* alleles was very obvious during oogenesis. Germ-line clones of the null allele *aPKC^{k06403}* failed to form an oocyte in 72% of the cases analyzed. By contrast, oocyte determination failed in only 6% of germ-line clones for any of the four new alleles, demonstrating that neither the loss of the kinase activity of aPKC nor the inability of aPKC to bind PAR-6 affect oocyte determination.

There are controversial reports about the involvement of aPKC and its phosphorylation targets in polarization of the oocyte at stages 9 and 10. Two papers claim that neither Lgl nor Crb are important for germ-line development (Benton and St Johnston, 2003; Doerflinger et al., 2006), but a recent paper reported that the localization of Staufen is abnormal in 47% of *aPKC^{k06403}* mutant oocytes at stages 9-10 and that these defects are most probably caused by the failure to phosphorylate Lgl (Tian and Deng, 2008). In our experiments, Staufen and Gurken localized normally in all oocytes mutant for any of the four hypomorphic *aPKC* alleles and in the vast majority of *aPKC^{k06403}* mutant oocytes at stage 9-10, which would suggest that there is no central function for aPKC in polarization of the oocyte at later stages of oogenesis.

Conclusions

We have described the molecular and biochemical properties and the mutant phenotypes of four hypomorphic alleles of *aPKC* encoding proteins that either fail to bind to PAR-6 or lack kinase activity. The reduced function of these alleles causes severe defects in apical-basal polarity in embryonic epithelia and neuroblasts, whereas oocyte determination and polarity of the follicle epithelium are nearly unaffected. Together, these data point to fundamental differences in the functioning of aPKC in these different tissues and they furthermore show that some functions of aPKC are independent of its kinase activity and of its ability to bind PAR-6.

Materials and Methods

Fly stocks and genetics

2R-69-30, *2R-141-24*, *2R-265-2* and *2R-417-13* alleles are derived from a mosaic screen for maternal effect embryonic lethal mutations that were induced on a chromosome carrying the P{FRT(w^{hs})}G13 (42B) FRT element (Luschnig et al., 2004) and were renamed *aPKC^{psu69}*, *aPKC^{psu141}*, *aPKC^{psu265}* and *aPKC^{psu417}* in this work after demonstrating that they are hypomorphic alleles of *aPKC*. Mutations in *aPKC^{psu}* flies (Luschnig et al., 2004) were identified by sequencing of PCR fragments encompassing the whole coding region of *aPKC* from genomic DNA of homozygous mutant or heterozygous flies. We furthermore used the null allele *aPKC^{k06403}* (Wodarz et al., 2000; Rolls et al., 2003) recombined onto the P{FRT(w^{hs})}G13 (42B) chromosome and the null allele *par-6^{Δ226}* (Petronczki and Knoblich, 2001) recombined onto the P{FRT(w^{hs})}9-2 (18E) chromosome. Df(2R)Jp1/CyO (Bloomington Drosophila Stock Center #3518) takes out the whole *aPKC* locus. For generation of germ-line clone embryos with the FLP-DFS technique, the appropriate *ovo^{D1}* stocks were used (Chou and Perrimon, 1992; Chou and Perrimon, 1996). For generation of genetically marked germ-line clones and follicle cell clones, appropriate FRT stocks carrying transgenes encoding green fluorescent protein (GFP) under control of the ubiquitin promoter were used.

Generation of antibodies against PAR-6 and Miranda

Antibodies against PAR-6 and Miranda were raised by injection of the keyhole limpet hemocyanin (KLH)-conjugated peptides HHQQAASNASTIMASDVKDGVLHL (PAR-6) and CSPPQKQVLKARNI (Miranda) into guinea pigs (Eurogentec, Herstal, Belgium).

Immunohistochemistry, TUNEL assay, electron microscopy and cuticle preparations

Embryos and ovaries were fixed in 4% formaldehyde and phosphate buffer pH 7.4. The primary antibodies used were rabbit anti-PKCζ C20 (Santa Cruz Biotechnology) 1:1000, rabbit anti-Baz (Wodarz et al., 1999) 1:1000, guinea-pig anti-PAR-6 1:1000, guinea-pig anti-Mira 1:1000, rabbit anti-Insc (Kraut and Campos-Ortega, 1996) 1:1000, mouse anti-Nrt BP106 (DSHB) 1:5, rat anti-DE-Cadherin, DCAD-2 (Uemura et al., 1996) (DSHB) 1:20, rat anti-Crb (U. Tepass) 1:500, rabbit anti-Dlg (Woods and Bryant, 1991) 1:1000, mouse anti-Grk 1D12 (DSHB), rabbit anti-Staufen (St Johnston et al., 1991) 1:500, mouse anti-Orb 4H8 (DSHB) 1:20, rat anti-Vasa (Tomancak et al., 1998) 1:5000, rabbit anti-active DRICE (Yoo et al., 2002) 1:5000. DNA was stained with YOYO-1 (Invitrogen). Secondary antibodies conjugated to Cy2, Cy3, Cy5 (Jackson Laboratories) and Alexa-Fluor-647 (Invitrogen) were used at 1:400. Images were taken on a Leica TCSNT confocal microscope or on a Zeiss LSM 510 Meta confocal microscope and processed using Adobe Photoshop. TUNEL assays, for detection of cell death in situ, were performed as described previously (Wang et al., 1999). Transmission electron microscopy was performed as described previously (Tepass and Hartenstein, 1994). Cuticle preparations were done as described previously (Wieschaus and Nüsslein-Volhard, 1986).

Western blots and immunoprecipitation

Methods were as described by Wodarz (Wodarz, 2008). For western analysis, the antibodies used were rabbit anti-PKCζ C20 (Santa Cruz Biotechnology) 1:2000, rabbit anti-phospho-PKCζ T410 (Santa Cruz Biotechnology) 1:1000, rabbit anti-BazpS980 (Krahn et al., 2009) 1:100, rabbit anti-GST (Sigma #G7781) 1:1000, and guinea-pig anti-PAR-6 1:2000. For immunoprecipitations, 2 μl of rabbit anti-GFP (Molecular Probes #A11122), 2 μl of guinea pig anti-PAR-6, 2 μl of the corresponding preimmune serum, 10 μl of rabbit anti-β-galactosidase (MP Biomedicals #55976) or 2 μl of rat anti-HA 3F10 (Roche) were added to cell lysate containing 500 μg of total protein from S2 cells in TNT (1% Triton X-100, 150 mM NaCl, 50 mM Tris-HCl pH 7.5) supplemented with protease inhibitors. Immune complexes were harvested using protein A/G-conjugated agarose (Roche), washed three times in TNT and boiled in 2× SDS sample buffer before SDS-PAGE and western blotting.

In vitro kinase assays

In vitro kinase assays were essentially performed as described previously (Lin et al., 2000). In brief, GFP-aPKC was immunoprecipitated from lysates of transfected S2 cells as described above. The beads were washed once in washing buffer (150 mM NaCl and 50 mM Tris-HCl pH 7.5) and twice in reaction buffer (20 mM Hepes, pH 7.5, 5 mM MgCl, 1 mM dithiothreitol). Immunoprecipitates were incubated for 1 hour at 30°C in reaction buffer containing 2 μg affinity purified GST-Baz, 250 μM ATP, 0.3 μCi [γ-^{32}P]ATP, 0.1 mM cantharidin and protease inhibitors. The reaction was terminated by addition of SDS sample buffer and samples were subjected to

SDS-PAGE. Phosphorylation was detected with PhosphorImager and quantified with Aida 2D Densitometry software. For non-radioactive kinase assays, phosphorylation of GST-Baz was determined by western blotting with the anti-BazpS980 phospho-specific antibody.

Generation of aPKC and Baz expression constructs
Details will be provided upon request.

Molecular dynamics simulations
ATP-binding free energy double differences $(G^{Mut.}{}_f - G^{Mut.}{}_{+ATP}) - (G^{WT}{}_f - G^{WT}{}_{+ATP})$ and folding free energy differences $(G^{Mut.}{}_u - G^{Mut.}{}_f) - (G^{WT}{}_u - G^{WT}{}_f)$ have been calculated from the thermodynamic cycle shown in Fig. 6B via the mutation free energy differences $G^{Mut.}{}_f - G^{WT}{}_f$, $G^{Mut.}{}_u - G^{WT}{}_u$ and $G^{Mut.}{}_{+ATP} - G^{WT}{}_{+ATP}$ in the folded, unfolded, and ATP-bound states, respectively. As models for the unfolded state, appropriately equilibrated tri- and penta-peptides were used with neutralized termini.

In all simulations, a cut-off of 1.07 nm for short-range Coulomb as well as Lennard-Jones forces was used. Particle-Mesh-Ewald with a grid spacing of 0.128 nm and an interpolation order of 4 was used for the long range electrostatics (Darden et al., 1993). A 300 K, 1 bar NpT ensemble using Parinello-Rahman pressure (τ_p=5 picoseconds) (Parrinello and Rahman, 1981; Nosé and Klein, 1983), V-rescale temperature coupling (τ_T=0.5 picoseconds) (Bussi et al., 2007), and a 2-femtosecond time step with the LINCS algorithm (Hess et al., 1997) was used. All simulations were carried out with the TIP3P water model (Jorgensen et al., 1983) and a 150 mM NaCl concentration. All simulations were carried out with the GROMACS software package (version 4) (Hess et al., 2008) using the AMBER99SB force field (Hornak et al., 2006) for the protein and the parameters for ATP and ions from Meagher et al. (Meagher et al., 2003) and Dang (Dang, 1995). All free energy calculations were carried out with the Crooks' Gaussian Intersection (CGI) scheme (Goette and Grubmüller, 2009) and a soft-core potential (Beutler et al., 1994) for all Lennard-Jones interconversions, with α=0.25. Fifty subsequent 50-picosecond thermodynamic integration simulations were carried out for each of the three mutations, and the obtained free energy differences and error estimates were calculated as described by Goette and Grubmüller (Goette and Grubmüller, 2009).

Starting from the crystal structure of the catalytic domain of human protein kinase Cι (chain A of PDB entry 1ZRZ (Messerschmidt et al., 2005)), with missing amino acids added (Fig. 6A), the system was equilibrated for 200 nanoseconds. Three point mutations, A272V, G328N and F404I, were constructed using WHATIF (Vriend, 1990) with subsequent energy minimization and 100 nanosecond equilibration. After the equilibration of the apo-enzyme structures, Mg²⁺-ATP was inserted, and the systems were further equilibrated for 50 nanoseconds.

The small missing loop element (446-455) was implemented via tconcoord (Seeliger et al., 2007; Seeliger and De Groot, 2008). Amino acids 532–555 were taken from the homologous structure 2I0E (Grodsky et al., 2006) (sequence identity 49%) with the respective amino acids mutated/inserted with WHATIF (Vriend, 1990). The resulting structure was then solvated, energy minimized, and slowly heated up from 20 K to 300 K while position restraining all non-modeled atoms. To enhance sampling, the system was then simulated for 1 nanosecond at 500 K with identical position restraints. From this trajectory, ten snapshots were used for simulated annealing simulations where the temperature was reduced from 500 K to 300 K within 1 nanosecond. A suitable starting structure for the subsequent production runs was obtained via principal component analysis (supplementary material Fig. S5). The Mg²⁺-ATP complex structure was modeled from the equilibrated ligand-free protein by root mean square fitting using the binding pocket of the Mg-GMPPNP-containing homologous structure 1DAY (Niefind et al., 1999). Stability of all simulations was monitored using the root mean square deviations (supplementary material Fig. S6).

References

Abdelilah-Seyfried, S., Cox, D. N. and Jan, Y. N. (2003). Bazooka is a permissive factor for the invasive behavior of discs large tumor cells in Drosophila ovarian follicular epithelia. *Development* **130**, 1927-1935.

Bachmann, A., Schneider, M., Theilenberg, E., Grawe, F. and Knust, E. (2001). Drosophila Stardust is a partner of Crumbs in the control of epithelial cell polarity. *Nature* **414**, 638-643.

Bello, B., Reichert, H. and Hirth, F. (2006). The brain tumor gene negatively regulates neural progenitor cell proliferation in the larval central brain of Drosophila. *Development* **133**, 2639-2648.

Benton, R. and St Johnston, D. (2003). Drosophila PAR-1 and 14-3-3 inhibit Bazooka/PAR-3 to establish complementary cortical domains in polarized cells. *Cell* **115**, 691-704.

Betschinger, J., Mechtler, K. and Knoblich, J. A. (2003). The Par complex directs asymmetric cell division by phosphorylating the cytoskeletal protein Lgl. *Nature* **422**, 326-330.

Betschinger, J., Eisenhaber, F. and Knoblich, J. A. (2005). Phosphorylation-induced autoinhibition regulates the cytoskeletal protein Lethal (2) giant larvae. *Curr. Biol.* **15**, 276-282.

Betschinger, J., Mechtler, K. and Knoblich, J. A. (2006). Asymmetric segregation of the tumor suppressor brat regulates self-renewal in Drosophila neural stem cells. *Cell* **124**, 1241-1253.

Beutler, T. C., Mark, A. E., van Schaik, R. C., Gerber, P. R. and van Gunsteren, W. F. (1994). Avoiding singularities and numerical instabilities in free energy calculations based on molecular simulations. *Chem. Phys. Lett.* **222**, 529-539.

Bilder, D., Schober, M. and Perrimon, N. (2003). Integrated activity of PDZ protein complexes regulates epithelial polarity. *Nat. Cell. Biol.* **5**, 53-58.

Bussi, G., Donadio, D. and Parrinello, M. (2007). Canonical sampling through velocity rescaling. *J. Chem. Phys.* **126**, 014101.

Chou, M. M., Hou, W., Johnson, J., Graham, L. K., Lee, M. H., Chen, C. S., Newton, A. C., Schaffhausen, B. S. and Toker, A. (1998). Regulation of protein kinase C zeta by PI 3-kinase and PDK-1. *Curr. Biol.* **8**, 1069-1077.

Chou, T. B. and Perrimon, N. (1992). Use of a yeast site-specific recombinase to produce female germline chimeras in Drosophila. *Genetics* **131**, 643-653.

Chou, T. B. and Perrimon, N. (1996). The autosomal FLP-DFS technique for generating germline mosaics in Drosophila melanogaster. *Genetics* **144**, 1673-1679.

Cowan, C. R. and Hyman, A. A. (2004). Asymmetric cell division in C. elegans: cortical polarity and spindle positioning. *Annu. Rev. Cell. Dev. Biol.* **20**, 427-453.

Cox, D. N., Seyfried, S. A., Jan, L. Y. and Jan, Y. N. (2001). Bazooka and atypical protein kinase C are required to regulate oocyte differentiation in the Drosophila ovary. *Proc. Natl. Acad. Sci. USA* **98**, 14475-14480.

Dang, L. X. (1995). Mechanism and thermodynamics of ion selectivity in aqueous solutions of 18-crown-6 ether: a molecular dynamics study. *J. Am. Chem. Soc.* **117**, 6954-6960.

Darden, T., York, D. and Pedersen, L. (1993). Particle mesh Ewald: an N log (N) method for Ewald sums in large systems. *J. Chem. Phys.* **98**, 10089-10092.

Doerflinger, H., Benton, R., Torres, I. L., Zwart, M. F. and St Johnston, D. (2006). Drosophila anterior-posterior polarity requires actin-dependent PAR-1 recruitment to the oocyte posterior. *Curr. Biol.* **16**, 1090-1095.

Goette, M. and Grubmüller, H. (2009). Accuracy and convergence of free energy differences calculated from nonequilibrium switching processes. *J. Comp. Chem.* **30**, 447-456.

Grawe, F., Wodarz, A., Lee, B., Knust, E. and Skaer, H. (1996). The Drosophila genes crumbs and stardust are involved in the biogenesis of adherens junctions. *Development* **122**, 951-959.

Grodsky, N., Li, Y., Bouzida, D., Love, R., Jensen, J., Nodes, B., Nonomiya, J. and Grant, S. (2006). Structure of the catalytic domain of human protein kinase C beta II complexed with a bisindolylmaleimide inhibitor. *Biochemistry* **45**, 13970-13981.

Harris, K. P. and Tepass, U. (2008). Cdc42 and Par proteins stabilize dynamic adherens junctions in the Drosophila neuroectoderm through regulation of apical endocytosis. *J. Cell Biol.* **183**, 1129-1143.

Harris, T. J. and Peifer, M. (2004). Adherens junction-dependent and -independent steps in the establishment of epithelial cell polarity in Drosophila. *J. Cell Biol.* **167**, 135-147.

Harris, T. J. and Peifer, M. (2005). The positioning and segregation of apical cues during epithelial polarity establishment in Drosophila. *J. Cell Biol.* **170**, 813-823.

Harris, T. J. and Peifer, M. (2007). aPKC controls microtubule organization to balance adherens junction symmetry and planar polarity during development. *Dev. Cell* **12**, 727-738.

Hess, B., Bekker, H., Berendsen, H. J. C. and Fraaije, J. G. E. M. (1997). LINCS: a linear constraint solver for molecular simulations. *J. Comp. Chem.* **18**, 1463-1472.

Hess, B., Kutzner, C., van der Spoel, D. and Lindahl, E. (2008). GROMACS 4: algorithms for highly efficient, load-balanced, and scalable molecular simulation. *J. Chem. Theor. Comp.* **4**, 435-447.

Hirai, T. and Chida, K. (2003). Protein kinase Czeta (PKCzeta): activation mechanisms and cellular functions. *J. Biochem.* **133**, 1-7.

Hirano, Y., Yoshinaga, S., Takeya, R., Suzuki, N. N., Horiuchi, M., Kohjima, M., Sumimoto, H. and Inagaki, F. (2005). Structure of a cell polarity regulator, a complex between atypical PKC and Par6 PB1 domains. *J. Biol. Chem.* **280**, 9653-9661.

Hirata, J., Nakagoshi, H., Nabeshima, Y. and Matsuzaki, F. (1995). Asymmetric segregation of the homeodomain protein Prospero during Drosophila development. *Nature* **377**, 627-630.

Hong, Y., Stronach, B., Perrimon, N., Jan, L. Y. and Jan, Y. N. (2001). Drosophila Stardust interacts with Crumbs to control polarity of epithelia but not neuroblasts. *Nature* **414**, 634-638.

Hornak, V., Abel, R., Okur, A., Strockbine, B., Roitberg, A. and Simmerling, C. (2006). Comparison of multiple amber force fields and development of improved protein backbone parameters. *Proteins Struct. Funct. Bioinfo.* **65**, 712-725.

Hurd, T. W., Gao, L., Roh, M. H., Macara, I. G. and Margolis, B. (2003). Direct interaction of two polarity complexes implicated in epithelial tight junction assembly. *Nat. Cell Biol.* **5**, 137-142.

Hurov, J. B., Watkins, J. L. and Piwnica-Worms, H. (2004). Atypical PKC phosphorylates PAR-1 kinases to regulate localization and activity. *Curr. Biol.* **14**, 736-741.

Hutterer, A., Betschinger, J., Petronczki, M. and Knoblich, J. A. (2004). Sequential roles of Cdc42, Par-6, aPKC, and Lgl in the establishment of epithelial polarity during Drosophila embryogenesis. *Dev. Cell* **6**, 845-854.

Huynh, J. R., Petronczki, M., Knoblich, J. A. and St Johnston, D. (2001). Bazooka and PAR-6 are required with PAR-1 for the maintenance of oocyte fate in *Drosophila*. *Curr. Biol.* **11**, 901-906.

Ikeshima-Kataoka, H., Skeath, J. B., Nabeshima, Y., Doe, C. Q. and Matsuzaki, F. (1997). Miranda directs Prospero to a daughter cell during Drosophila asymmetric divisions. *Nature* **390**, 625-629.

Izumi, Y., Hirose, T., Tamai, Y., Hirai, S., Nagashima, Y., Fujimoto, T., Tabuse, Y., Kemphues, K. J. and Ohno, S. (1998). An atypical PKC directly associates and colocalizes at the epithelial tight junction with ASIP, a mammalian homologue of caenorhabditis elegans polarity protein PAR-3. *J. Cell Biol.* **143**, 95-106.

Joberty, G., Petersen, C., Gao, L. and Macara, I. G. (2000). The cell-polarity protein Par6 links Par3 and atypical protein kinase C to Cdc42. *Nat. Cell Biol.* **2**, 531-539.

Johansson, A., Driessens, M. and Aspenstrom, P. (2000). The mammalian homologue of the caenorhabditis elegans polarity protein PAR-6 is a binding partner for the Rho GTPases cdc42 and rac1. *J. Cell Sci.* **113**, 3267-3275.

Johnson, K. and Wodarz, A. (2003). A genetic hierarchy controlling cell polarity. *Nat. Cell. Biol.* **5**, 12-14.

Jorgensen, W. L., Chandrasekhar, J., Madura, J. D., Impey, R. W. and Klein, M. L. (1983). Comparison of simple potential functions for simulating liquid water. *J. Chem. Phys.* **79**, 926.

Kempkens, O., Medina, E., Fernandez-Ballester, G., Ozuyaman, S., Le Bivic, A., Serrano, L. and Knust, E. (2006). Computer modelling in combination with in vitro studies reveals similar binding affinities of Drosophila Crumbs for the PDZ domains of Stardust and DmPar-6. *Eur. J. Cell Biol.* **85**, 753-767.

Knoblich, J. A. (2008). Mechanisms of asymmetric stem cell division. *Cell* **132**, 583-597.

Knoblich, J. A., Jan, L. Y. and Jan, Y. N. (1995). Asymmetric segregation of Numb and Prospero during cell division. *Nature* **377**, 624-627.

Knust, E. and Bossinger, O. (2002). Composition and formation of intercellular junctions in epithelial cells. *Science* **298**, 1955-1959.

Krahn, M. P., Egger-Adam, D. and Wodarz, A. (2009). PP2A antagonizes phosphorylation of Bazooka by PAR-1 to control apical-basal polarity in dividing embryonic neuroblasts. *Dev. Cell* **16**, 901-908.

Kraut, R. and Campos-Ortega, J. A. (1996). inscuteable, a neural precursor gene of Drosophila, encodes a candidate for a cytoskeleton adaptor protein. *Dev. Biol.* **174**, 65-81.

Kuchinke, U., Grawe, F. and Knust, E. (1998). Control of spindle orientation in Drosophila by the Par-3-related PDZ- domain protein Bazooka. *Curr. Biol.* **8**, 1357-1365.

Kusakabe, M. and Nishida, E. (2004). The polarity-inducing kinase Par-1 controls Xenopus gastrulation in cooperation with 14-3-3 and aPKC. *EMBO J.* **23**, 4190-4201.

Le Good, J. A., Ziegler, W. H., Parekh, D. B., Alessi, D. R., Cohen, P. and Parker, P. J. (1998). Protein kinase C isotypes controlled by phosphoinositide 3-kinase through the protein kinase PDK1. *Science* **281**, 2042-2045.

Lee, C. Y., Robinson, K. J. and Doe, C. Q. (2006a). Lgl, Pins and aPKC regulate neuroblast self-renewal versus differentiation. *Nature* **439**, 594-598.

Lee, C. Y., Wilkinson, B. D., Siegrist, S. E., Wharton, R. P. and Doe, C. Q. (2006b). Brat is a Miranda cargo protein that promotes neuronal differentiation and inhibits neuroblast self-renewal. *Dev. Cell* **10**, 441-449.

Lemmers, C., Michel, D., Lane-Guermonprez, L., Delgrossi, M. H., Medina, E., Arsanto, J. P. and Le Bivic, A. (2004). CRB3 binds directly to Par6 and regulates the morphogenesis of the tight junctions in mammalian epithelial cells. *Mol. Biol. Cell* **15**, 1324-1333.

Lin, D., Edwards, A. S., Fawcett, J. P., Mbamalu, G., Scott, J. D. and Pawson, T. (2000). A mammalian Par-3-Par-6 complex implicated in CdC42/Rac1 and aPKC signalling and cell polarity. *Nat. Cell Biol.* **2**, 540-547.

Lu, B., Rothenberg, M., Jan, L. Y. and Jan, Y. N. (1998). Partner of Numb colocalizes with Numb during mitosis and directs Numb asymmetric localization in Drosophila neural and muscle progenitors. *Cell* **95**, 225-235.

Luschnig, S., Moussian, B., Krauss, J., Desjeux, I., Perkovic, J. and Nusslein-Volhard, C. (2004). An F1 genetic screen for maternal-effect mutations affecting embryonic pattern formation in Drosophila melanogaster. *Genetics* **167**, 325-342.

Meagher, K. L., Redman, L. T. and Carlson, H. A. (2003). Development of polyphosphate parameters for use with the AMBER force field. *J. Comp. Chem.* **24**, 1016-1025.

Messerschmidt, A., Macieira, S., Velarde, M., Bädeker, M., Benda, C., Jestel, A., Brandstetter, H., Neuefeind, T. and Blaesse, M. (2005). Crystal structure of the catalytic domain of human atypical protein kinase C-iota reveals interaction mode of phosphorylation site in turn motif. *J. Mol. Biol.* **352**, 918-931.

Mirouse, V., Christoforou, C. P., Fritsch, C., St Johnston, D. and Ray, R. P. (2009). Dystroglycan and perlecan provide a basal cue required for epithelial polarity during energetic stress. *Dev. Cell* **16**, 83-92.

Müller, H. A. and Wieschaus, E. (1996). armadillo, bazooka, and stardust are critical for early stages in formation of the zonula adherens and maintenance of the polarized blastoderm epithelium in Drosophila. *J. Cell Biol.* **134**, 149-163.

Nagai-Tamai, Y., Mizuno, K., Hirose, T., Suzuki, A. and Ohno, S. (2002). Regulated protein-protein interaction between aPKC and PAR-3 plays an essential role in the polarization of epithelial cells. *Genes Cells* **7**, 1161-1171.

Nelson, W. J. (2003). Adaptation of core mechanisms to generate cell polarity. *Nature* **422**, 766-774.

Newton, A. C. (1995). Protein kinase C: structure, function, and regulation. *J. Biol. Chem.* **270**, 28495-28498.

Niefind, K., Puetter, M., Guerra, B., Issinger, O. G. and Schomburg, D. (1999). GTP plus water mimic ATP in the active site of protein kinase CK2. *Nat. Struct. Biol.* **6**, 1100-1103.

Noda, Y., Kohjima, M., Izaki, T., Ota, K., Yoshinaga, S., Inagaki, F., Ito, T. and Sumimoto, H. (2003). Molecular recognition in dimerization between PB1 domains. *J. Biol. Chem.* **278**, 43516-43524.

Nosé, S. and Klein, M. (1983). Constant pressure molecular dynamics for molecular systems. *Mol. Phys.* **50**, 1055-1076.

Parrinello, M. and Rahman, A. (1981). Polymorphic transitions in single crystals: A new molecular dynamics method. *J. Appl. Phys.* **52**, 7182.

Peterson, F. C., Penkert, R. R., Volkman, B. F. and Prehoda, K. E. (2004). Cdc42 regulates the Par-6 PDZ domain through an allosteric CRIB-PDZ transition. *Mol. Cell* **13**, 665-676.

Petronczki, M. and Knoblich, J. A. (2001). DmPAR-6 directs epithelial polarity and asymmetric cell division of neuroblasts in *Drosophila*. *Nat. Cell. Biol.* **3**, 43-49.

Plant, P. J., Fawcett, J. P., Lin, D. C., Holdorf, A. D., Binns, K., Kulkarni, S. and Pawson, T. (2003). A polarity complex of mPar-6 and atypical PKC binds, phosphorylates and regulates mammalian Lgl. *Nat. Cell. Biol.* **5**, 301-308.

Rhyu, M. S., Jan, L. Y. and Jan, Y. N. (1994). Asymmetric distribution of numb protein during division of the sensory organ precursor cell confers distinct fates to daughter cells. *Cell* **76**, 477-491.

Rolls, M. M., Albertson, R., Shih, H. P., Lee, C. Y. and Doe, C. Q. (2003). Drosophila aPKC regulates cell polarity and cell proliferation in neuroblasts and epithelia. *J. Cell Biol.* **163**, 1089-1098.

Schneider, M., Khalil, A. A., Poulton, J., Castillejo-Lopez, C., Egger-Adam, D., Wodarz, A., Deng, W. M. and Baumgartner, S. (2006). Perlecan and Dystroglycan act at the basal side of the Drosophila follicular epithelium to maintain epithelial organization. *Development* **133**, 3805-3815.

Schober, M., Schaefer, M. and Knoblich, J. A. (1999). Bazooka recruits Inscuteable to orient asymmetric cell divisions in Drosophila neuroblasts. *Nature* **402**, 548-551.

Schuldt, A. J., Adams, J. H., Davidson, C. M., Micklem, D. R., Haseloff, J., St Johnston, D. and Brand, A. H. (1998). Miranda mediates asymmetric protein and RNA localization in the developing nervous system. *Genes Dev.* **12**, 1847-1857.

Seeliger, D. and De Groot, B. L. (2008). tCONCOORD-GUI: Visually supported conformational sampling of bioactive molecules. *J. Comp. Chem.* **30**, 1160-1166.

Seeliger, D., Haas, J. and de Groot, B. L. (2007). Geometry-based sampling of conformational transitions in proteins. *Structure* **15**, 1482-1492.

Shen, C. P., Jan, L. Y. and Jan, Y. N. (1997). Miranda is required for the asymmetric localization of Prospero during mitosis in Drosophila. *Cell* **90**, 449-458.

Smith, C. A., Lau, K. M., Rahmani, Z., Dho, S. E., Brothers, G., She, Y. M., Berry, D. M., Bonneil, E., Thibault, P., Schweisguth, F. et al. (2007). aPKC-mediated phosphorylation regulates asymmetric membrane localization of the cell fate determinant Numb. *EMBO J.* **26**, 468-480.

Sotillos, S., Diaz-Meco, M. T., Caminero, E., Moscat, J. and Campuzano, S. (2004). DaPKC-dependent phosphorylation of Crumbs is required for epithelial cell polarity in Drosophila. *J. Cell Biol.* **166**, 549-557.

Spana, E. P. and Doe, C. Q. (1995). The prospero transcription factor is asymmetrically localized to the cell cortex during neuroblast mitosis in Drosophila. *Development* **121**, 3187-3195.

St Johnston, D., Beuchle, D. and Nusslein-Volhard, C. (1991). Staufen, a gene required to localize maternal RNAs in the Drosophila egg. *Cell* **66**, 51-63.

Suzuki, A. and Ohno, S. (2006). The PAR-aPKC system: lessons in polarity. *J. Cell Sci.* **119**, 979-987.

Suzuki, A., Yamanaka, T., Hirose, T., Manabe, N., Mizuno, K., Shimizu, M., Akimoto, K., Izumi, Y., Ohnishi, T. and Ohno, S. (2001). Atypical protein kinase C is involved in the evolutionarily conserved par protein complex and plays a critical role in establishing epithelia-specific junctional structures. *J. Cell Biol.* **152**, 1183-1196.

Suzuki, A., Hirata, M., Kamimura, K., Maniwa, R., Yamanaka, T., Mizuno, K., Kishikawa, M., Hirose, H., Amano, Y., Izumi, N. et al. (2004). aPKC acts upstream of PAR-1b in both the establishment and maintenance of mammalian epithelial polarity. *Curr. Biol.* **14**, 1425-1435.

Tanentzapf, G. and Tepass, U. (2003). Interactions between the crumbs, lethal giant larvae and bazooka pathways in epithelial polarization. *Nat. Cell. Biol.* **5**, 46-52.

Tanentzapf, G., Smith, C., McGlade, J. and Tepass, U. (2000). Apical, lateral, and basal polarization cues contribute to the development of the follicular epithelium during Drosophila oogenesis. *J. Cell Biol.* **151**, 891-904.

Tepass, U. (1996). Crumbs, a component of the apical membrane, is required for zonula adherens formation in primary epithelia of Drosophila. *Dev. Biol.* **177**, 217-225.

Tepass, U. and Knust, E. (1993). Crumbs and stardust act in a genetic pathway that controls the organization of epithelia in Drosophila melanogaster. *Dev. Biol.* **159**, 311-326.

Tepass, U. and Hartenstein, V. (1994). The development of cellular junctions in the Drosophila embryo. *Dev. Biol.* **161**, 563-596.

Tepass, U., Theres, C. and Knust, E. (1990). crumbs encodes an EGF-like protein expressed on apical membranes of Drosophila epithelial cells and required for organization of epithelia. *Cell* **61**, 787-799.

Tian, A. G. and Deng, W. M. (2008). Lgl and its phosphorylation by aPKC regulate oocyte polarity formation in Drosophila. *Development* **135**, 463-471.

Tomancak, P., Guichet, A., Zavorszky, P. and Ephrussi, A. (1998). Oocyte polarity depends on regulation of gurken by Vasa. *Development* **125**, 1723-1732.

Uemura, T., Oda, H., Kraut, R., Hayashi, S., Kotaoka, Y. and Takeichi, M. (1996). Zygotic Drosophila E-cadherin expression is required for processes of dynamic epithelial cell rearrangement in the Drosophila embryo. *Genes Dev.* **10**, 659-671.

Vaccari, T. and Ephrussi, A. (2002). The fusome and microtubules enrich Par-1 in the oocyte, where it effects polarization in conjunction with Par-3, BicD, Egl, and dynein. *Curr. Biol.* **12**, 1524-1528.

Vriend, G. (1990). WHAT IF: a molecular modeling and drug design program. *J. Mol. Graph.* **8**, 52-56.

Wang, Q., Hurd, T. W. and Margolis, B. (2004). Tight junction protein Par6 interacts with an evolutionarily conserved region in the amino terminus of PALS1/stardust. *J. Biol. Chem.* **279**, 30715-30721.

Wang, S. L., Hawkins, C. J., Yoo, S. J., Muller, H. A. and Hay, B. A. (1999). The Drosophila caspase inhibitor DIAP1 is essential for cell survival and is negatively regulated by HID. *Cell* **98**, 453-463.

Wieschaus, E. and Nüsslein-Volhard, C. (1986). Looking at embryos. In *Drosophila, a Practical Approach* (ed. D. B. Roberts), pp. 199-227. Oxford: IRL Press.

Wilson, M. I., Gill, D. J., Perisic, O., Quinn, M. T. and Williams, R. L. (2003). PB1 domain-mediated heterodimerization in NADPH oxidase and signaling complexes of atypical protein kinase C with Par6 and p62. *Mol. Cell* **12**, 39-50.

Wirtz-Peitz, F., Nishimura, T. and Knoblich, J. A. (2008). Linking cell cycle to asymmetric division: Aurora-A phosphorylates the Par complex to regulate Numb localization. *Cell* **135**, 161-173.

Wodarz, A. (2002). Establishing cell polarity in development. *Nat. Cell. Biol.* **4**, E39-E44.

Wodarz, A. (2005). Molecular control of cell polarity and asymmetric cell division in Drosophila neuroblasts. *Curr. Opin. Cell Biol.* **17**, 475-481.

Wodarz, A. (2008). Extraction and immunoblotting of proteins from embryos. In *Drosophila: Methods and Protocols*, vol. 420 (ed. C. Dahmann), pp. 335-345. Totowa, NJ: Humana Press.

Wodarz, A. and Huttner, W. B. (2003). Asymmetric cell division during neurogenesis in Drosophila and vertebrates. *Mech. Dev.* **120**, 1297-1309.

Wodarz, A., Hinz, U., Engelbert, M. and Knust, E. (1995). Expression of Crumbs confers apical character on plasma membrane domains of ectodermal epithelia of Drosophila. *Cell* **82**, 67-76.

Wodarz, A., Ramrath, A., Kuchinke, U. and Knust, E. (1999). Bazooka provides an apical cue for Inscuteable localization in Drosophila neuroblasts. *Nature* **402**, 544-547.

Wodarz, A., Ramrath, A., Grimm, A. and Knust, E. (2000). Drosophila atypical protein kinase C associates with Bazooka and controls polarity of epithelia and neuroblasts. *J. Cell Biol.* **150**, 1361-1374.

Woods, D. F. and Bryant, P. J. (1991). The discs-large tumor suppressor gene of Drosophila encodes a guanylate kinase homolog localized at septate junctions. *Cell* **66**, 451-464.

Yamanaka, T., Horikoshi, Y., Suzuki, A., Sugiyama, Y., Kitamura, K., Maniwa, R., Nagai, Y., Yamashita, A., Hirose, T., Ishikawa, H. et al. (2001). PAR-6 regulates aPKC activity in a novel way and mediates cell-cell contact-induced formation of the epithelial junctional complex. *Genes Cells* **6**, 721-731.

Yamanaka, T., Horikoshi, Y., Sugiyama, Y., Ishiyama, C., Suzuki, A., Hirose, T., Iwamatsu, A., Shinohara, A. and Ohno, S. (2003). Mammalian Lgl forms a protein complex with PAR-6 and aPKC independently of PAR-3 to regulate epithelial cell polarity. *Curr. Biol.* **13**, 734-743.

Yoo, S. J., Huh, J. R., Muro, I., Yu, H., Wang, L., Wang, S. L., Feldman, R. M., Clem, R. J., Muller, H. A. and Hay, B. A. (2002). Hid, Rpr and Grim negatively regulate DIAP1 levels through distinct mechanisms. *Nat. Cell. Biol.* **4**, 416-424.